Fluorescent nanocarriers targeting VCAM-1 for early detection of senescent endothelial cells

Eugenia Belcastro, Asad Ur Rehman, Lamia Remila, Sin-Hee Park, Dal Seong Gong, Nicolas Anton, Cyril Auger, Olivier Lefebvre, Jacky G Goetz, Mayeul Collot, et al.

ELSEVIER

Nanomedicine: Nanotechnology, Biology, and Medicine
xx (xxxx) xxx

nanomedicine
Nanotechnology, Biology, and Medicine

nanomedjournal.com

Fluorescent nanocarriers targeting VCAM-1 for early detection of senescent endothelial cells

Eugenia Belcastro[a,1], Asad Ur Rehman[b,1], Lamia Remila[a], Sin-Hee Park[a], Dal Seong Gong[a], Nicolas Anton[a,b], Cyril Auger[a], Olivier Lefebvre[c], Jacky G. Goetz[c], Mayeul Collot[d], Andrey S. Klymchenko[d], Thierry F. Vandamme[a,b], Valérie B. Schini-Kerth[a,*]

[a]*INSERM (French National Institute of Health and Medical Research), UMR 1260, Regenerative Nanomedicine, Faculty of Pharmacy*
[b]*University of Strasbourg, CNRS, CAMB UMR 7199, Strasbourg, France*
[c]*INSERM UMR 1109, Tumor Biomechanics*
[d]*CNRS UMR 7213, Laboratory of Biophotonics and Pharmacology, University of Strasbourg, Strasbourg, France*

Revised 29 January 2021

Abstract

Endothelial senescence has been identified as an early event in the development of endothelial dysfunction, a hallmark of cardiovascular disease. This study developed theranostic nanocarriers (NC) decorated with VCAM-1 antibodies (NC-VCAM-1) in order to target cell surface VCAM-1, which is overexpressed in senescent endothelial cells (ECs) for diagnostic and therapeutic purposes. Incubation of Ang II-induced premature senescent ECs or replicative senescent ECs with NC-VCAM-1 loaded with lipophilic fluorescent dyes showed higher fluorescence signals than healthy EC, which was dependent on the NC size and VCAM-1 antibodies concentration, and not observed following masking of VCAM-1. NC loaded with omega 3 polyunsaturated fatty acid (NC-EPA:DHA 6:1) were more effective than native EPA:DHA 6:1 to prevent Ang II-induced VCAM-1 and p53 upregulation, and SA-β-galactosidase activity in coronary artery segments. These theranostic NC might be of interest to evaluate the extent and localization of endothelial senescence and to prevent pro-senescent endothelial responses.

Key words: Nanocarriers; Endothelial senescence and dysfunction; VCAM-1; Omega 3 polyunsaturated fatty acid

Cardiovascular diseases (CVDs) are the leading cause of death in the developed world and represent an immense clinical burden.[1] Atherothrombosis, a chronic and progressive inflammatory disease,[2] has been identified as the major contributor to the pathogenesis of CVDs including acute coronary syndrome and stroke.[3]

Although clinical scores, such as that derived from the Framingham Heart Study, are useful to evaluate the cardiovascular risk of patients, they may lose predictive value in the large segment of the population at intermediate risk.[4] Thus, there is a crucial need for novel diagnostic tools to identify early molecular changes associated with atherogenesis and to assess noninvasively the benefit of therapies, and also for new targeted and specific therapies. Recent findings have emphasized the potential role of nanoparticles, as promising tools for treatment of vascular disease, including atherothrombosis and its associated complications.[5] The recent development of ultrabright theranostic nanoparticles that may simultaneously act as carriers of both imaging payloads and therapeutic agents, has great promises for the future of personalized medicine.[6]

The atherogenesis process starts before childhood with the appearance of early lesions of atherosclerosis, which can progress into mature plaques impeding blood flow and optimal perfusion of target organs, and, ultimately, trigger an atherothrombotic event. Interestingly, the atherogenesis process is not a generalized alteration of the cardiovascular system but is targeting well-defined arterial sites at risk such as bifurcations and curvatures including the carotid and aorta-renal bifurcations.[7,8] Such

No conflict of interest.
This research did not receive any specific grant from funding agencies in the public, commercial, or not-for-profit sectors.
* Corresponding author at: UMR1260 INSERM, University of Strasbourg, Faculty of Pharmacy, F-67401 Illkirch, France.
E-mail address: valerie.schini-kerth@unistra.fr (V.B. Schini-Kerth).
[1] Equal contribution of these authors.

https://doi.org/10.1016/j.nano.2021.102379
1549-9634/

atheroprone areas are characterized by an early development of endothelial dysfunction most likely as a consequence of their particular local flow behavior involving disturbed flow and low shear versus the atheroprotective areas characterized by laminar flow and high shear.[3,9] Indeed, high shear stress is a pivotal trigger of endothelial cell (ECs) protective mechanisms especially the formation of nitric oxide (NO), a potent vasodilator and inhibitor of atherothrombotic responses. Thus, ECs at athero-susceptible arterial sites are unlikely to protect adequately the arterial wall thereby accelerating the development of atherosclerotic lesions.[3]

Recent investigations support the concept that endothelial senescence is a determinant event leading to the development of endothelial dysfunction.[10,11] Cellular senescence is characterized by the hallmark marker senescence-associated β galactosidase activity, an irreversible cell cycle arrest,[12] and the induction of a pro-inflammatory senescence-associated secretory phenotype (SASP)[13,14,15] with increased expression of VCAM-1, MCP-1 and tissue factor, and down-regulation of the endothelial formation of NO, and is induced by pro-oxidant stimuli such as angiotensin II (Ang II) and elevated glucose concentration.[16,17] Increased numbers of senescent ECs have been observed overlying plaques in the human coronary artery[18] and the aortic arch.[19] The fact that overexpression of the senescence marker p53 selectively in the endothelium blunted NO formation and promoted endothelial dysfunction in rat aortic rings,[20] suggests that endothelial senescence leads to endothelial dysfunction. Among vasoprotective treatments, omega 3 polyunsaturated fatty acids (PUFAs) including eicosapentaenoic acid (EPA) and docosahexaenoic acid (DHA) have been shown to protect the cardiovascular system, in part, by causing a sustained endothelial formation of NO. Indeed, our previous studies indicated that EPA:DHA 6:1 is a superior omega 3 PUFA formulation to induce endothelium-dependent vasorelaxation in coronary artery rings, to cause eNOS activation in ECs, and to improve aging-related endothelial dysfunction.[21,22]

Thus, the main objective of the present study was to target endothelial senescence by taking advantage of a unique feature of the cell membrane of senescent ECs, the increased cell surface expression of VCAM-1. For this purpose, a core-shell nanoemulsions carrier decorated with antibodies (Abs) targeting VCAM-1 was generated and loaded with either lipophilic red or near-infrared (NIR) fluorescent dyes to enable detection of senescent ECs using fluorescence imaging or EPA:DHA 6:1 for delivery and regeneration of the protective endothelial function.

Methods

A detailed description of the experimental protocols and chemicals is provided in the Supplementary material.

Preparation of maleimide-decorated nanoemulsions: grafting of anti-VCAM-1 antibody and fluorescent dye loading

Oil and aqueous phases were prepared separately and heated at 90 °C for 30 min. Oil phase consists of polymer and 1% of dye based on Nile Red (NR668)[23] or NIR cyanine with a bulky counterion tetraphenylborate (Cy5.5-TPB)[24] dissolved in oil (Labrafac WL®), while the aqueous phase used was distilled water. 100 mg of maleimide modified polymer (synthesis described in supporting information) and 25 mg of dye/Labrafac WL® were mixed in a vial (4 ml). Then, 800 μl of hot distilled water was added and this mixture was homogenized by vortex for 30 s to obtain a primary emulsion and finally homogenized by ultrasonication to produce nanoemulsions (technical details are reported in the *Supplementary information* section). In some experiments, the non-functionalized nanocarriers were formulated with EPA:DHA 6:1 instead of Labrafac WL® as dispersed phase and distilled water as continuous phase, without any fluorescent probe. Furthermore, different amounts of the anti-VCAM-1 Ab were added into the diluted nanoemulsions to study the effect of increasing concentrations of the antibody on the extent of grafting. After Ab addition, the nanoemulsions were incubated for 24 h at 4-6 °C to cause attachment of the Ab onto the maleimide functions at the surface of the nanocarriers (NC-VCAM-1). The maleimide-decorated nanoemulsions, without grafting of the antibody at the surface of the nanocarriers (NC), were also used as a control formulation for the study.

Endothelial cell culture and preparation of coronary artery rings

ECs were isolated from freshly harvested porcine left circumflex coronary arteries using type I collagenase as described previously,[25] and cultured in MCDB 131 medium containing 15% fetal calf serum, fungizone (2.5 μg/ml), penicillin (100 U/ml), streptomycin (100 μg/ml), and 5 L-glutamine (2 mM). ECs at passage 1 were exposed to serum-free culture medium for 2 h before the addition of Ang II to induce premature senescence. ECs passaged at a ratio of 1:3 until passage 3 to induce replicative senescence were also studied.[26] Coronary artery segments were incubated in RPMI without serum for 1 h before the addition of Ang II. Thereafter, they were embedded in FSC22 Frozen section medium and frozen.

Detection of senescence-associated β-galactosidase activity (SA-β-gal)

Senescence-associated β-galactosidase activity was assessed in porcine coronary artery segments by staining with X-gal solution as previously reported.[27]

Immunofluorescence studies and physicochemical characterization of nanocarriers

For immunofluorescence histochemistry, ECs and isolated healthy porcine coronary artery rings were evaluated using a Leica SP2 UV DM Irbe confocal laser-scanning microscope with 20× or 63×/OIL CS objectives. Quantification of fluorescence levels was performed with macros developed with Image J software. Nanocarrier physicochemical characteristics were evaluated for the chemical optimization, such as the nanocarrier average size, the different amounts of Abs, the PEG/PEG-antibody ratio, the temperature stability, the use of different fluorescent probes and the targeting efficiency.

Statistical analysis

Data are expressed as means ± SEM. Statistical analysis was assessed by one-way analysis of variance followed by Bonferroni's Multiple Comparison post hoc test using GraphPad Prism

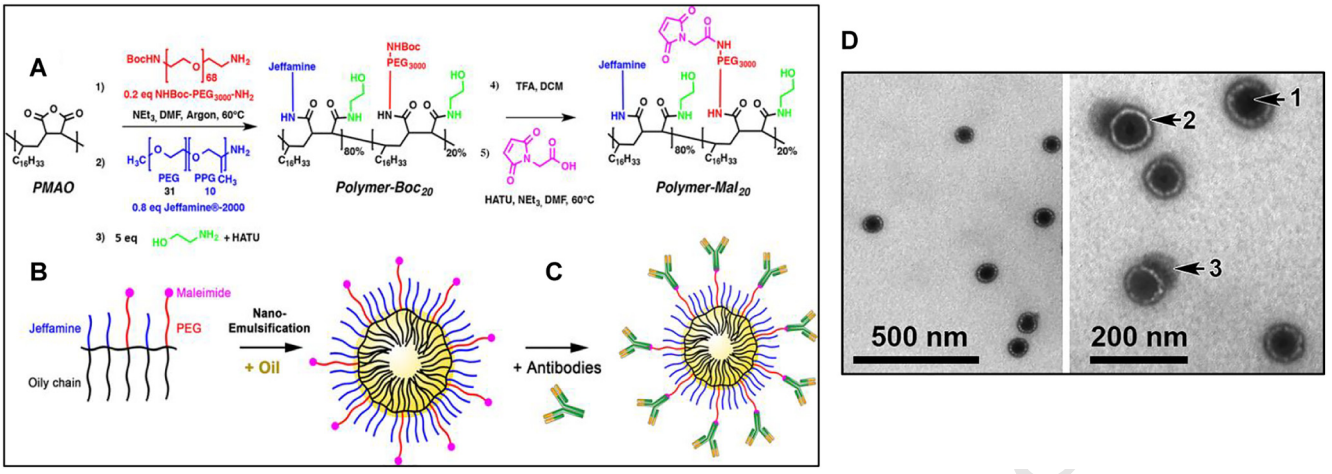

Figure 1. Design and chemical development of targeting lipid nanocarriers. **(A)** Synthesis of the maleimide decorated polymer, starting by a reaction between PMAO and Boc-NH-PEG3000-NH_2 on 20% of the anhydride functions of the polymer (1); the remaining 80% of the anhydride functions of the polymer were then reacted with Jeffamine-2000 (2); afterwards, ethanolamine was used to neutralize the unreacted carboxylic groups (3); then the deprotection of the amino functions of the Polymer-Boc_{20} was performed (4) followed by coupling of amino groups with the maleimidoacetic acid (5) resulting in the formation of Polymer-Mal_{20}. **(B)** Formation of nanoemulsions by ultrasonication method and **(C)** grafting of VCAM-1 Abs with the available maleimide functions on the surface of the nanocarriers. **(D)** TEM characterization of nanoemulsions formed by using polymer dissolved in 1% Cy5.5-TPB solution in Labrafac® as oil phase and distilled water as aqueous phase with spherical shape.

(Version 5). Group differences were considered statistically significant at $P < 0.05$.

Results

Synthesis of the amphiphilic polymer and evaluation of the structure by 1H NMR analysis

As a polymeric platform, PMAO is an alternated polymer (average M_n 30,000-50,000) with a repeating unit composed of a hydrophobic hydrocarbon chain (C_{18}) and a succinic anhydride function. As illustrated, an amphiphilic polymer (Polymer-Boc_{20}) was first synthesized through a reaction of PMAO with an amino-PEG_{3000} bearing a protected amino function (Boc-NH-PEG_{3000}-NH_2) on 20% of the anhydride functions (Figure 1, *A*). The remaining 80% of anhydride functions were then reacted with Jeffamine®2000, an amino/methoxy terminated PEG/PPG (poly(ethylene glycol)/poly(propylene glycol)) copolymer, to reduce the polymer hydrophobicity. Then the deprotection of the amino functions of Polymer-Boc_{20} was performed followed by coupling of the amino groups with the maleimidoacetic acid to result in the formation of Polymer-Mal_{20} (Figure 1, *A*). The progress of the reaction, the structure of the polymer was studied by performing NMR at each step of the synthesis of this amphiphilic polymer derivative (reported in Supplementary Information Figure S1). In Figure S1, ethanol is visible (not dry enough after dialysis) as well as the peak of NHBoc. The integration and comparison to the CH_3 of PEG show functionalization with PEG-NHBoc close to 20% (equal to 1.72 while 20% would correspond to a value of 1.8). This result proves that the ratio expected between non-functional and functional PEG chains is obtained. This value of 80% is confirmed with the integration of the NMR peak of the Me function (terminating the Jeffamines chains), as indicated in Figure S1. Then, the disappearance of the NHBoc peak in Figure S2 clearly confirmed the deprotection has been efficiently done. Comparison of two spectra is reported in Figure S3. On the other hand, NMR spectra with maleimide addition appear to be identical to the those after deprotection of Boc (Figure S4), likely due to screening of the numerous PEG chains present in these macromolecules. To summarize, NMR results have confirmed the attachment of Jeffamine® 2000 (80%) and PEG-NH_2 (20%) with the polymer network and confirmed the gradual building of the functional polymer.

Preparation of targeted fluorescent lipid nanocarriers

The multifunctional lipid nanocarriers were formulated by ultrasonication method. To render them fluorescent, their core was loaded with highly lipophilic dyes (NR668 or Cy5.5-TPB).[22,23] While NR668, operating in the red spectral range, is well adapted for fluorescence microscopy studies, the NIR dye Cy5.5-TPB is more suitable for in vivo and tissue imaging and they both display high stability against dye leakage in biological media.[28] The amphiphilic polymer derivative described above was used to stabilize the nanoemulsions and also to provide the facility to functionalize the nanocarriers after their formulation. During the formation of nanodroplets the amphiphilic polymer is expected to reorganize in such a way that the hydrophobic hydrocarbon chains remain in the apolar interior of the nanodroplets (oil phase) whereas the hydrophilic part of the polymer (J-2000 and maleimide-decorated PEG chains) is exposed towards the interface of the droplets (towards aqueous phase), as previously described.[29] This provides active maleimide functions at the surface of the nanodroplets which will ensure an anchorage of the VCAM-Abs, because the polymer is a part of the nanocarrier "shell" (Figure 1, *B*). Antibody decoration is performed by incubation of the functional maleimide-decorated

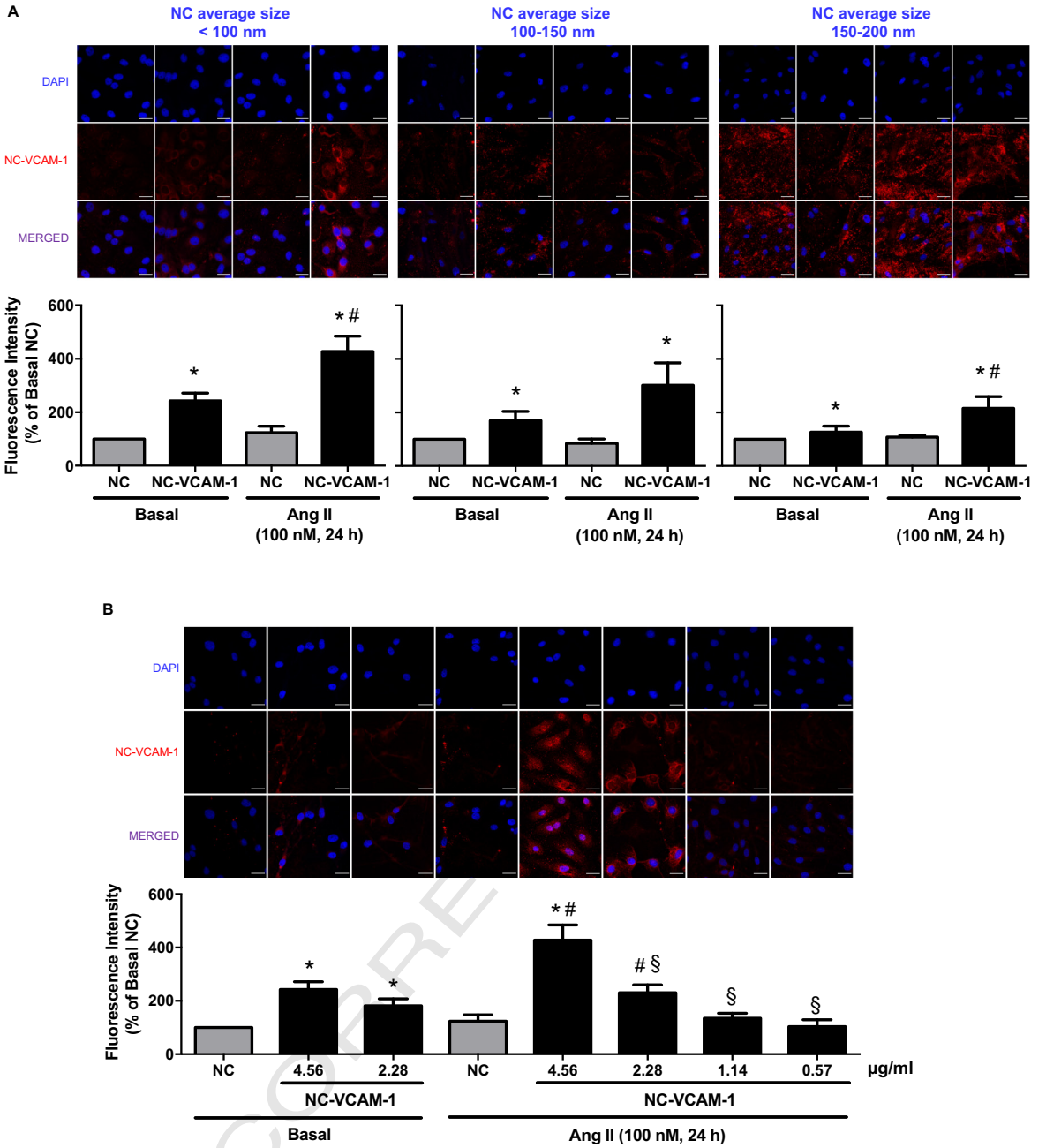

Figure 2. Optimization and evaluation of the theranostic potential of nanocarriers targeting surface VCAM-1 in a model of premature senescence. ECs are incubated with Ang II for 24 h to induce premature senescence and subsequently with either nanocarriers (NC) or nanocarriers decorated with VCAM-1 Abs (NC-VCAM-1) for 1 h. Experimental conditions tested NC with different diameters **(A)**, different concentrations of the anti-VCAM-1 Abs **(B)**, different storage temperatures **(C)**, and containing a specific designed lipophilic dye (NR668 or Cy5.5-TPB) **(D)**. NC and NC-VCAM-1 fluorescence staining appears in red and nuclei are stained with DAPI (blue). Results are shown as representative of immunofluorescence staining (upper panels) and corresponding cumulative data (lower panels). Data are expressed as mean ± SEM of n = 3-9 D. $^{*}P < 0.05$ vs respective NC, $^{\#}P < 0.05$ vs respective NC-VCAM-1, $^{\S}P < 0.05$ vs Ang II NC-VCAM-1 4.56 µg/ml. Original magnification, 63×. Scale bar = 20 µm.

nanoemulsions with the solution of anti-VCAM-1 Abs attaching the nanodroplets surface (Figure 1, *C*), giving rise to functionalized nanocarriers. As a control formulation, nanoemulsions with a polymer without having the Boc-NH-PEG_{3000}-NH_2 component, i.e., PMAO:J-2000, 1:1 respectively were prepared. This formulation was prepared to compare the average hydrodynamic diameter as well as the surface charge on the droplets with the ones obtained with maleimide decorated nanocarriers.

Characterization of size and surface charge

The nanocarriers loaded with fluorescent probes (NR668 or Cy5.5-TPB) were characterized by DLS analysis. The average

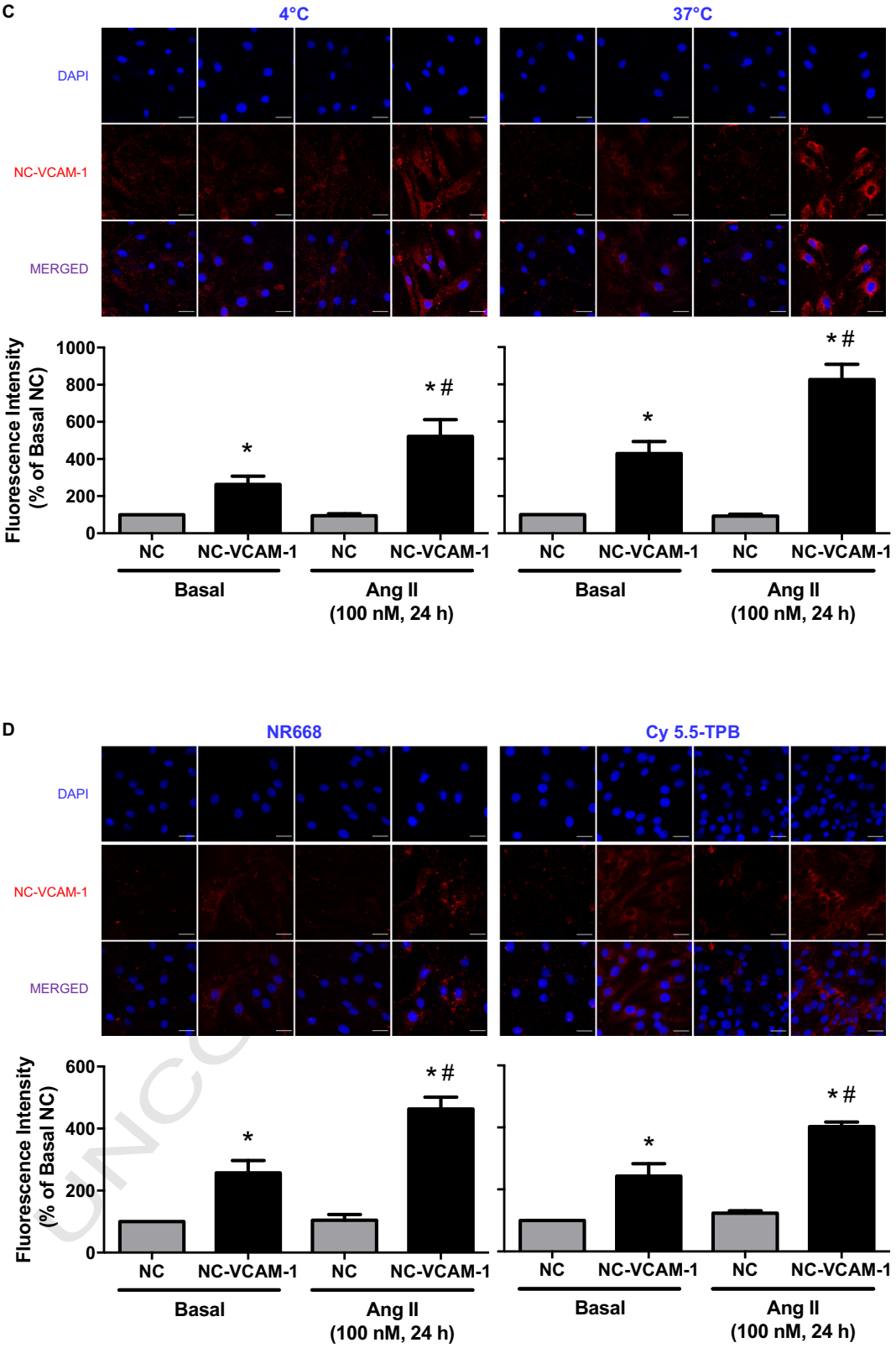

Figure 2. (*continued*).

hydrodynamic diameter of the maleimide-decorated nanoemulsions was 96 ± 7 nm (n = 10). The hydrodynamic diameters obtained for nanocarriers developed by using Labrafac®, omega 3 EPA:DHA 6:1 oil and corn oil as dispersed phase were 96 nm, 80 nm and 190 nm, respectively. This difference is likely related to the nature of this oil impacting on the spontaneous emulsification process.[30] In the other two cases the average hydrodynamic diameters of the nanodroplets were below 100 nm, the optimal size for theranostic applications.[31] The average size of the nanodroplets obtained in the case of control formulation (PMAO: J2000 1:1) was considerably larger (around 160 nm) as compared to the maleimide-decorated nanodroplets. According to zeta-potential measurements, the surface charge on the nanoemulsion droplets, in the control formulation, was negative (−39 mV±1, n = 3) and the surface charge on the maleimide-decorated nanodroplets was positive and ranged from 10 to 15 mV, regardless of the nature of the oil used to formulate the nanocarriers (n = 8 for NR668/Cy5.5 TPB in Labrafac®, n = 3 for omega 3 EPA:DHA 6:1, n = 3 for corn oil). This change in the surface charge from negative to positive is most likely due to complete saturation of the carboxylic groups, followed by grafting of maleimide on the available sites.

TEM analysis of these nanocarriers (containing Cy5.5-TPB) is reported in Figure 1, *D*. The results confirmed the morphology and average size of the nanoemulsions given by DLS, i.e. below 100 nm. In addition, micrographs disclosed structural information, indeed coherent with the one expected: oil core (arrow 1 in Figure 1, *D*) is surrounded by a polymer shell (arrow 2). In some particles the presence of amorphous polymer can be observed (arrow 3). Interestingly, the bright aspect of the polymer shell is related to a pure and concentrated material, and this can be explained by the process itself. Initially the polymer is homogeneously solubilized in the oil phase, and then the emulsification process induces its concentration at the interface, making a concentrated shell. In some cases, excess of polymer (arrow 3) has induced amorphous domains. TEM pictures have confirmed a nanocarrier structure in line with the one eventually expected.

Optimization and evaluation of theranostics nanocarriers in in vitro senescence models

Size

In order to determine the importance of the size of VCAM-1 Ab-decorated nanocarriers, lipid nanocarriers with hydrodynamic diameters below 100 nm, 100-150 nm and 150-200 nm ranges were prepared by changing the time of formulation exposition to the ultrasonication process, and tested using control and Ang II-induced premature endothelial cell senescence. The highest fluorescence signal in cells was observed with the nanocarriers having sizes below 100 nm compared to those having sizes ranging from 100 to 150 nm and 150-200 nm (Figure 2, *A*). Thus, the targeting efficiency increased with the decrease in the size of the VCAM-1 Ab-decorated nanocarriers. Therefore, the lipid nanocarriers having diameter size below 100 nm were selected and used for further experiments. It is interesting to note that a better targeting efficiency is obtained for smaller particles. Indeed, for a similar amount of polymer and oils forming the nanocarriers, two different sizes mean a difference in particle number (concentration) and in the particle surface area. Thus, for the smaller particles, the particle concentration and surface area exposing specific ligands should be higher, which should favor targeting properties. In addition, smaller particles diffuse faster, allowing faster ligand/receptor interaction.

Different concentrations of anti-VCAM-1 antibodies

To find the optimum concentration of the Abs linked to the maleimide active sites at the surface of the nanocarriers for targeting, different concentrations of the anti-VCAM-1 Abs were tested and analyzed. Higher fluorescence signals were obtained with the formulation with the highest antibody concentration (4.56 μg/ml) in Ang II-induced endothelial cell senescence whereas low levels were observed in control cells (Figure 2, *B*), indicating that the targeting was directly dependent on the amount of VCAM-1 Abs decorating the nanocarriers. All further experiments were performed with NC-VCAM-1 generated with anti-VCAM-1 Abs at a concentration of 4.56 μg/ml.

Different temperature and encapsulated dye

To further characterize the targeting of the formulations and validate their stability, the role of the temperature was assessed. The fluorescent VCAM-1 Abs decorated nanocarriers targeted Ang II-induced senescent ECs within 1 h, at both 4 °C and 37 °C (body temperature) with minimal off-target cell surface interactions (Figure 2, *C*). Nanocarriers labeled with specially designed lipophilic derivatives of dyes either NR668 or Cy5.5-TPB were bright enough to allow the fine tracking of interactions with biological systems (Figure 2, *D*). Altogether, these results indicate that the different temperatures and fluorescent probes can be used to image active targeting of cells by the lipid nanocarriers.

Specific targeting of NC-VCAM-1 in premature and replicative senescence ECs

The targeting specificity of fluorescent VCAM-1 Abs decorated nanocarriers at 37 °C was evaluated by competition experiments using a VCAM-1 Ab to mask the VCAM-1 antigen. Nanocarriers decorated with VCAM-1 Abs strongly stained Ang II-induced senescent ECs and replicative senescence ECs (passage 3, Figure 3. *A*, *B*) whereas no such effects were observed following pretreatment of the cells with a VCAM-1 Ab demonstrating their uniqueness to selectively target membrane surface VCAM-1.

Protective effect of theranostics NC-EPA:DHA 6:1 in native endothelium of coronary artery segments

Since all investigations were performed with cultured ECs, experiments evaluated the protective effect of the omega 3 EPA:DHA 6:1 formulation and corn oil on Ang II-induced premature senescence in coronary artery segments, and to assess the impact of nanoencapsulation of the two oils. Exposure of coronary artery segments to Ang II upregulated the expression level of VCAM-1 and the senescence marker p53, and increased SA-β-gal activity predominantly in the endothelium (Figure. 4, *A*, *B*, *C*). The EPA:DHA 6:1 treatment significantly reduced the stimulatory effect of

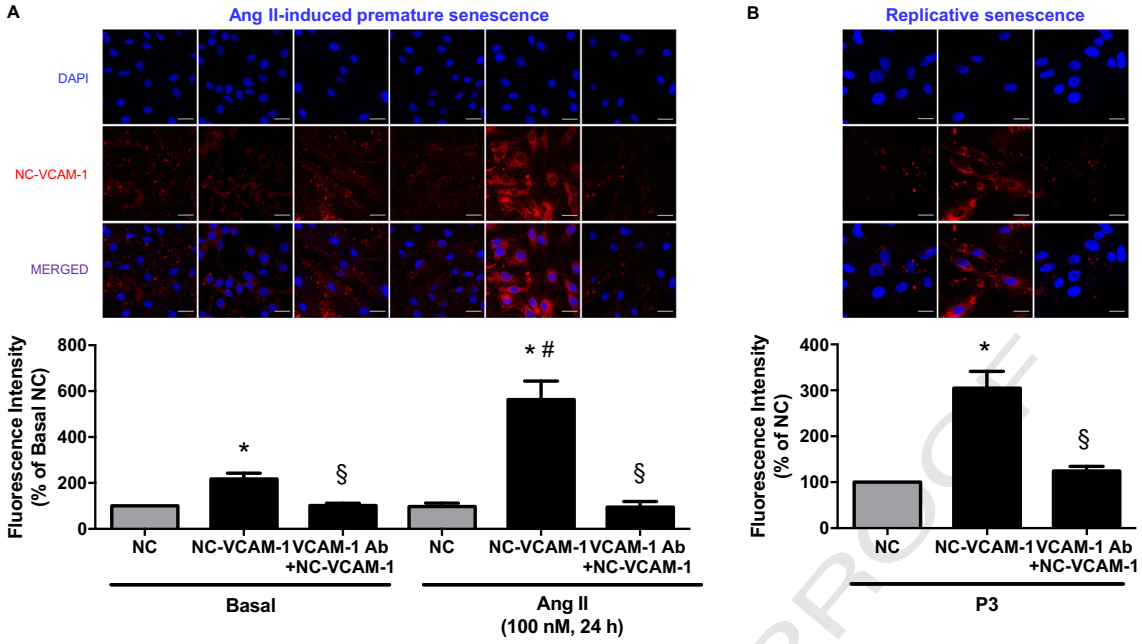

Figure 3. Selective targeting of the VCAM-1 decorated nanocarriers to premature and replicative senescent ECs. Nanocarriers decorated with VCAM-1 Abs (NC-VCAM-1) strongly stain ECs following their exposed to Ang II for 24 h to induce premature senescence **(A)**, and ECs at passage 3 (P3, replicative senescence) **(B)**. The targeting potential of NC-VCAM-1 is prevented by the previous exposure of ECs to the VCAM-1 Ab. NC and NC-VCAM-1 fluorescence staining appears in red and nuclei are stained with DAPI (blue). Results are shown as representative of immunofluorescence staining (upper panels) and corresponding cumulative data (lower panels). Data are expressed as mean ± SEM of n = 3-4. $^{*}P < 0.05$ vs respective NC, $^{\#}P < 0.05$ vs Basal NC-VCAM-1, $^{\S}P < 0.05$ vs respective NC-VCAM-1. Original magnification, 63×. Scale bar = 20 μm.

Ang II on VCAM-1 and SA-β-gal activity and reduced that on p53, which, however, did not reach statistical significance (Figure 4, *A*, *B*, *C*). The corn oil treatment blunted the stimulatory effect of Ang II on SA-β-gal activity and did not significantly affect that on VCAM-1and p53 (Figure 4, *A*, *B*, *C*). NC-EPA:DHA 6:1 markedly and significantly prevented Ang II-induced VCAM-1 and p53 upregulation in the endothelium of coronary artery segments, compared to the NC-CORN OIL (Figure 5, *A*, *B*). NC-EPA:DHA but not NC-CORN OIL also slightly but significantly reduced the VCAM-1 and p53 expression levels in control coronary artery segments (Figure 5, *A*, *B*).

Discussion

Atherosclerosis underlying major cardiovascular diseases, is a silent killer, which cannot be easily detected at an early stage by current imaging methods. Since the induction of endothelial senescence is thought to promote the development of endothelial dysfunction, an early event in the atherogenesis process, endothelial senescence appears to be an interesting target for both preventive and therapeutic interventions.[9,26,32,33]The major findings of the present study indicate the ability of nanocarriers decorated with VCAM-1 Abs and loaded with lipophilic fluorescent dyes to selectively and specifically target VCAM-1 overexpressed at the surface membrane of cultured senescent ECs compared to healthy ECs. They further show that nanoencapsulation of the vasoprotective omega 3 formulation EPA:DHA 6:1 is associated with enhanced inhibition of pro-atherosclerotic and pro-senescence responses in the native endothelium of isolated coronary arteries. Thus, fluorescent nanocarriers targeting a senescence-associated cell surface protein appear to be an attractive strategy to restore the protective endothelial function on the vascular system.

A low-grade inflammatory response is involved in the atherogenesis process affecting initially the endothelium with the appearance at the cell surface of several pro-atherothrombotic molecules including adhesion molecules that are tightly regulated both spatially and temporally.[3,34] Thus, these novel cell surface molecules are interesting targets for innovative diagnostics and therapeutics approaches in atherogenesis. Among potential candidates, VCAM-1 appears to be of particular interest since it is involved in the development of early atherosclerotic lesions[35,36] and has been observed on the endothelial cell surface of atheroprone areas before the onset of visible structural changes,[34] and increased levels of VCAM-1 expression have been associated with senescent ECs overlaying human atherosclerotic plaques.[18]

To date, several approaches have been described to image VCAM-1 and other cell adhesion molecules expression using radiolabeled antibodies,.[37,38] However, these agents usually result in modest target-to-background ratios,[37,38] limiting their use for in vivo cardiovascular imaging. Therefore, there is a need to develop alternative methods for imaging, ideally with improved sensitivity and resolution. Recently, nanoparticles have attracted a lot of interest as potential therapeutics, diagnostics, and theranostics due to their ability to target in a specific manner to the site of disease and to reduce the therapeutic load and, hence, side effects. The nanometric size of these materials and their surface functionalization

characteristics preclude them from being readily cleared through the kidneys and decelerate the opsonization mechanism, thereby extending circulation in blood.[39]

Targeted nanoparticles like polymeric nanoparticles (e.g., PLGA), liposomes and nanoemulsions, have been shown to specifically accumulate in ECs, and suggested to be used for imaging or drug delivery applications.[5] In comparison to the other nanocarriers, nanoemulsions (the system used in the current study) are particularly attractive as drug delivery vehicles because of their non-toxic components, high loading capacity, biodegradability, good stability, low manufacturing cost and their potential to encapsulate hydrophilic, lipophilic, as well as amphiphilic drugs.[40–44] Such a system is a dispersion of two immiscible liquids (water-in-oil or oil-in-water), stabilized by a surfactant, which is a isotropically clear and thermo-dynamically stable liquid solution, usually with droplet diameter within the range of 10-500 nm.[30,45,46] However, it is not easy to chemically modify the surface of the nanoemulsions due to the challenges involved in the stabilization of the interface. Recent findings demonstrate that when the oil phase containing the polymer is in contact with the aqueous phase, the polymer PMAO as well as its derivatives with Jeffamine polyetheramines (J-1000 & J-2000), shows the ability to migrate at the oil–water interface and produce stable oil-in-water nanoemulsions in the absence of an organic solvent as well as surfactant.[29] In the current study, a strategy to functionalize nanoemulsions with antibodies based on PMAO polymer has been developed. Chemical modification of PMAO, by performing a systematic reaction of Jeffamine polyetheramine (Jeffamine® M2070) and a polyethylene glycol (PEG)-containing compound terminated by a reactive maleimide on each anhydride function of the polymer has been made. The nanoemulsions are then developed using this newly synthesized polymer, with some PEG presenting maleimide at the surface of the nanodroplets to react with the cysteine function of the anti-VCAM-1 antibody, by ensuring a strong anchorage of the ligands since it will be a part of the nanocarriers as a "shell". The use of Jeffamine®2000 and PEG in this system, has great significance because the PEG-chains not only create steric repulsion among the neighboring nanodroplets and improve the interfacial stabilization but also have a well-recognized ability to i) reduce the uptake of the nanoemulsions by the immune system (after in vivo administration) and ii) inhibit the opsonization and phagocytosis processes, normally observed with conventional nanoemulsions, which in turn increases the circulation time of nanoemulsions in the body.[47,48] Another important

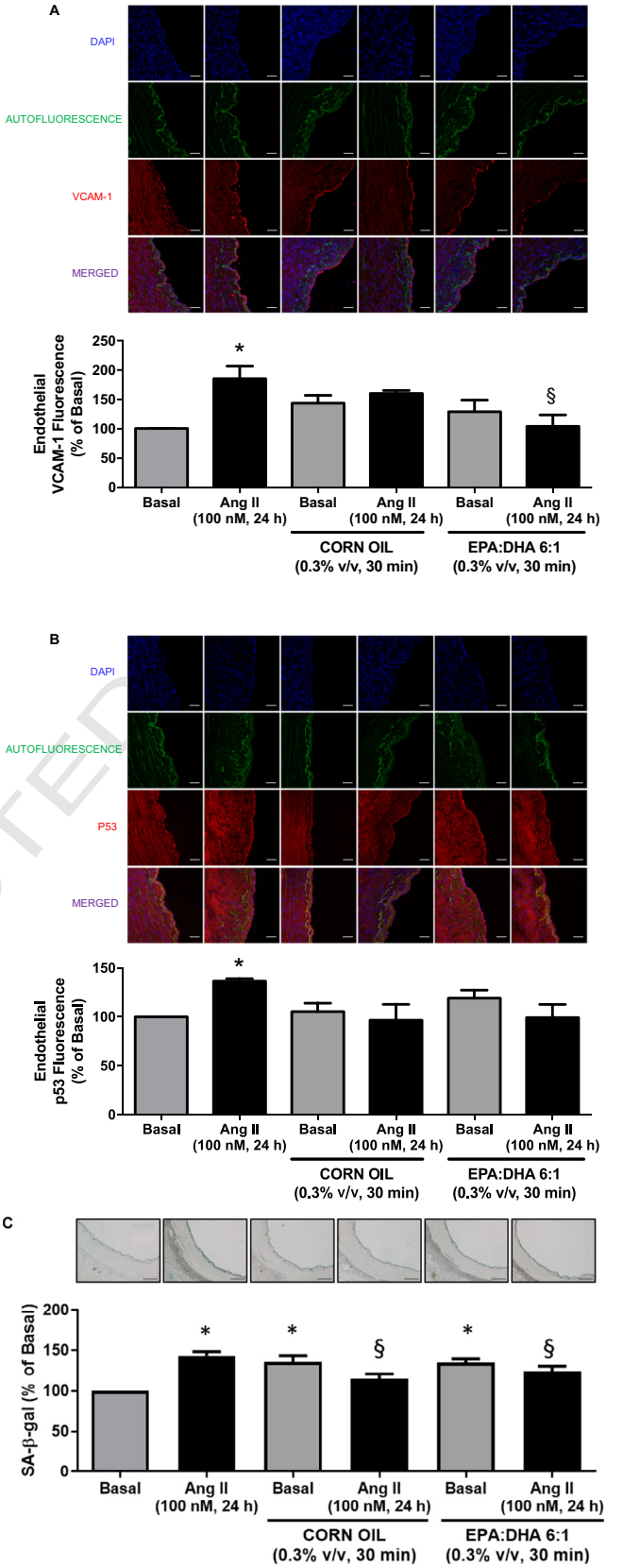

Figure 4. Native EPA:DHA 6:1 prevents the Ang II-induced up-regulation of VCAM-1 and SA-β-gal activity in the endothelium of coronary artery segments. Segments were either untreated, or exposed to CORN OIL or EPA:DHA 6:1 for 30 min before the addition of Ang II for 24 h. Thereafter, VCAM-1 and p53 signals were assessed by immunofluorescence, and SA-β-gal activity using X-gal. Representative images show VCAM-1 **(A)** and p53 **(B)** staining in red, nuclei in blue and autofluorescence in green (upper panels), and SA-β-gal activity (**C**, upper panels) and corresponding cumulative data of the endothelial signal (lower panels). Data are expressed as mean ± SEM of $n = 3$-4. $^{*}P < 0.05$ vs basal, $^{\S}P < 0.05$ vs Ang II. Original magnification, 20×. Scale bar = 50 μm **(A, B)**. Original magnification, 10×. Scale bar = 200 μm **(C)**.

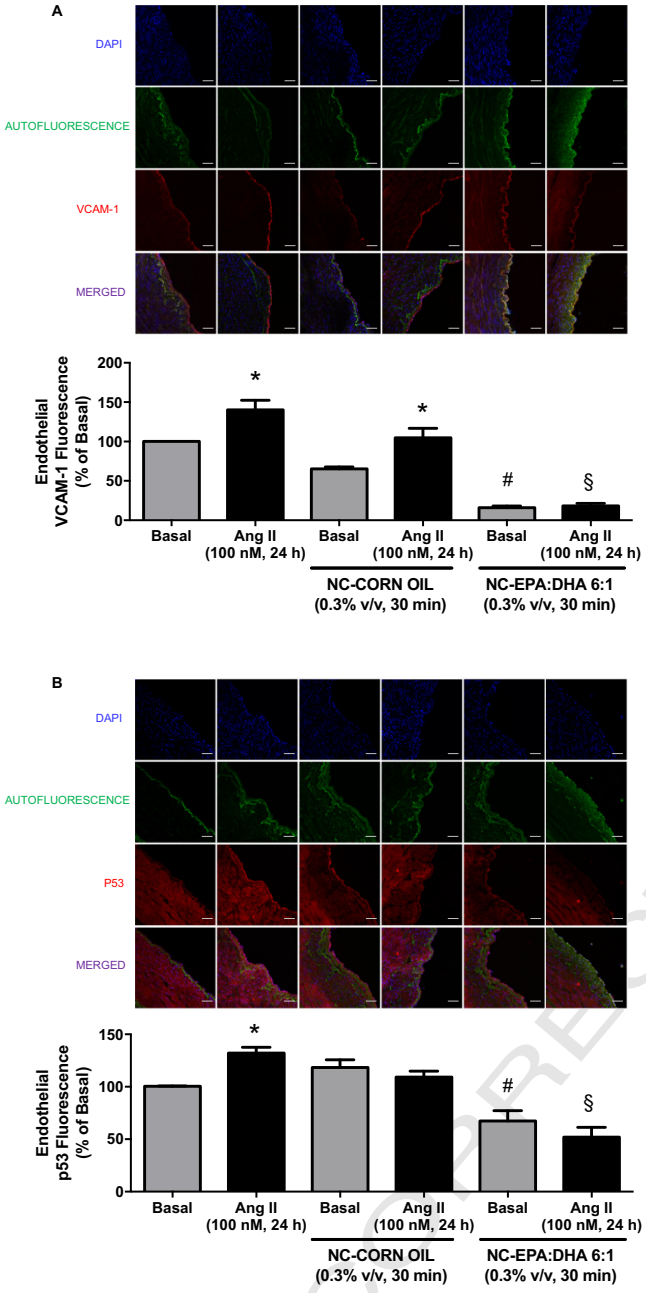

Figure 5. NC-EPA:DHA 6:1 strongly prevent the Ang II-induced up-regulation of VCAM-1 and p53 immunofluorescence signals in the endothelium of coronary artery segments. Segments were either untreated, or exposed to NC-CORN OIL or NC-EPA:DHA 6:1 for 30 min before the addition of Ang II for 24 h. Thereafter, the expression levels of VCAM-1 and p53 were assessed by immunofluorescence. Representative confocal immunofluorescence images showing VCAM-1 **(A)** and p53 **(B)** staining in red, nuclei in blue and autofluorescence in green (upper panels), and corresponding cumulative data of the endothelial signal (lower panels). Data are expressed as mean ± SEM of $n = 3$. $^{*}P < 0.05$ vs respective basal, $^{\#}P < 0.05$ vs untreated basal, $^{\S}P < 0.05$ vs Ang II. Original magnification, 20×. Scale bar = 50 μm.

chemical feature of this formulation is the type of fluorescent probe used. The probes studied, namely NR668 and Cy5.5-TPB, are specially designed to be highly lipophilic, resistant to dye leakage in biological media[28] and can be highly concentrated without excessive decrease of the fluorescence quantum yield.[23,24,49–52] As a result, nanocarriers are ultrabright and allow fine tracking of their interactions with biological systems.[23,24,49,50]

The biological evaluation of the fluorescent nanocarriers targeting VCAM-1 was assessed in vitro in premature and replicative senescent cultured ECs[26,33] and ex vivo in senescent native endothelium of isolated porcine coronary arteries. The nanoemulsion formulation has been optimized in relation to the size of the nanodroplets, which has an important impact on their interaction with living cells and also on the number of functional sites,[31,52] and the amount of the antibody to be attached to the maleimide groups available at the surface of the nanodroplets, which influences the efficient targeting of the targets.[39] These studies indicate that nanocarriers with average size below 100 nm and the highest antibody concentration tested (4.56 μg/ml) showed maximum fluorescence signals in senescent compared to healthy ECs, indicating that the targeting was directly dependent on the amount of VCAM-1 Abs decorating the nanocarriers. The targeting of senescent ECs by the nanocarriers is observed rapidly within 1 h, pronounced at body temperature and with minimal off-target cell surface interactions, and similar with the two fluorescent probes.

Among vasoprotective treatments, the omega 3 PUFAs, including EPA and DHA, have emerged as an attractive therapy to protect the cardiovascular system, by improving the endothelial function.[21] The beneficial effect of the omega 3 treatment is critically dependent on the purity level of the EPA and DHA, the EPA:DHA ratio, and also on the ability to protect the highly sensitive double bonds within their structures against oxidization.[21] Indeed, highly purified EPA:DHA 6:1 is a superior formulation than pure EPA, pure DHA and other EPA:DHA ratio including 1:1, causing a sustained endothelial formation of NO in cultured ECs and isolated artery rings including the human mammary artery.[21,53] The oral daily intake of EPA:DHA 6:1 has shown antihypertensive and improvement of the endothelial function in Ang II-treated rats, and has improved aging-related endothelial dysfunction by normalizing vascular levels of oxidative stress and restoring the endothelial formation of NO.[22] Such findings are in good agreement with those of the REDUCE-IT clinical trial indicating that the intake of pure EPA (4 g) provided about a 25% additional reduction in major adverse cardiovascular events in patients with elevated cardiovascular risk treated with a statin.[54] Therefore, the present study has evaluated the effect of EPA:DHA 6:1 compared to that of corn oil, an isocaloric "control" lipid, both in the native form and after loading in non-functionalized nanocarriers on the Ang II-induced activation of the native endothelium using coronary artery segments. The Ang II treatment caused the appearance of pronounced VCAM-1 and p53 signals and increased SA-β-gal activity predominantly in the endothelium highlighting the particular susceptibility of the endothelium in the arterial wall towards pathological stimuli.[55] The stimulatory effect of Ang II on the endothelial VCAM-1 and p53 signals was reduced to a greater extent by the nanoencapsulated EPA:DHA 6:1 compared to the native omega-3 form, and also compared to nanoencapsulated and native corn oil. Thus these ex vivo investigations indicate a therapeutic potential of nanocarriers containing EPA:

DHA 6:1 in the core to reach sufficient levels to restore the key protective endothelial function.

In conclusion, the present findings indicate the efficiency of fluorescent nanocarriers decorated with VCAM-1 Abs to selectively and specifically target VCAM-1 overexpressed at the membrane surface of cultured senescent ECs. They further indicate that nanoencapsulation of the vasoprotective and highly sensitive to oxidation EPA:DHA 6:1 leads to a greater beneficial effect towards the Ang II-induced dysfunction of native endothelium ex vivo. Additional in vivo studies are required to provide evidence of their monitoring and regenerative potentials of pathological endothelium overlying areas at risk. Ultimately, the developed platform could be applied to other targets, making it a useful scaffold for the development of novel targeted therapeutics and/or diagnostic tools.

Acknowledgments

We thank Romain Vauchelles (Laboratoire de Bioimagerie et Pathologie, CNRS UMR 7021) for support on microscopy and developing imageJ scripts, and Said Amissi and Ali Mroueh (INSERM UMR 1260, Regenerative Nanomedicine, Faculty of Pharmacy) for participation in the collection of data.

Appendix A. Supplementary data

Supplementary data to this article can be found online at https://doi.org/10.1016/j.nano.2021.102379.

References

1. World Health Organization. World Health Organization. https://www.who.int/news-room/fact-sheets/detail/the-top-10-causes-of-death.
2. Libby P. The vascular biology of atherosclerosis. In: Brunwald E, Zipes DP, Libby P, editors. *Heart disease: a textbook of cardiovascular medicine*. 6th edition. Philadelphia, PA: WB Saunders; 2001. p. 995-1009.
3. Libby P. Inflammation in atherosclerosis. *Nature* 2002;**420**:868-74.
4. Libby P, Ridker PM. Inflammation and atherosclerosis: role of C-reactive protein in risk assessment. *Am J Med* 2004;**116**(suppl 6):A:9S-16S.
5. Flores AM, Ye J, Jarr KU, Hosseini-Nassab N, Smith BR, Leeper NJ. Nanoparticle therapy or vascular diseases. *ATVB* 2019;**39**(4):635-46.
6. Theek B, Rizzo LY, Ehling J, Kiessling F, Lammers T. The theranostic path to personalized nanomedicine. *Clin Transl Imaging* 2014;**2**(1):66-76.
7. Benjamin EJ, Muntner P, Alonso A, Bittencourt MS, Callaway CW, Carson AP, et al. Heart disease and stroke statistics—2019 update: a report from the American Heart Association. *Circulation* 2019;**139**(10):e56-e528.
8. Suo J, Ferrara DE, Sorescu D, Guldberg RE, Taylor WR, Giddens DP. Hemodynamic shear stresses in mouse aortas: implications for atherogenesis. *ATVB* 2007;**27**(2):346-351.
9. Warboys CM, de Luca A, Amini N, Luong L, Duckles H, Hsiao S, et al. Disturbed flow promotes endothelial senescence via a p53-dependent pathway. *ATVB* 2014;**34**:985-95.
10. Heitzer T, Schlinzig T, Krohn K, Meinertz T, Munzel T. Endothelial dysfunction, oxidative stress, and risk of cardiovascular events in patients with coronary artery disease. *Circulation* 2001;**104**(22):2673-2678.
11. North BJ, Sinclair DA. The intersection between aging and cardiovascular disease. *Circ Res* 2012;**110**:1097-108.
12. McHugh D, Gil J. Senescence and aging: causes, consequences, and therapeutic avenues. *J Cell Biol* 2018;**217**:65-77.
13. Childs BG, Baker DJ, Wijshake T, Conover CA, Campisi J, van Deursen JM. Senescent intimal foam cells are deleterious at all stages of atherosclerosis. *Science* 2016;**354**:472-7.
14. Childs BG, Li H, van Deursen JM. Senescent cells: a therapeutic target for cardiovascular disease. *J Clin Invest* 2018;**128**:1217-28.
15. Childs BG, Durik M, Baker DJ, van Deursen JM. Cellular senescence in aging and age-related disease: from mechanisms to therapy. *Nat Med* 2015;**21**(12):1424-35.
16. Matsui-Hirai H, Hayashi T, Yamamoto S, Ina K, Maeda M, Kotani H, et al. Dose-dependent modulatory effects of insulin on glucose-induced endothelial senescence in vitro and in vivo: a relationship between telomeres and nitric oxide. *J Pharmacol Exp Ther* 2011;**337**:591-9.
17. Abdul-Ghani MA, Norton L, Defronzo RA. Role of sodium-glucose cotransporter 2 (SGLT 2) inhibitors in the treatment of type 2 diabetes. *Endocr Rev* 2011;**32**:515-31.
18. Minamino T, Miyauchi H, Yoshida T, Ishida Y, Yoshida H, Komuro I. Endothelial cell senescence in human atherosclerosis: role of telomere in endothelial dysfunction. *Circulation* 2002;**105**:1541-4.
19. Vasile E, Tomita Y, Brown LF, Kocher O, Dvorak HF. Differential expression of thymosin beta-10 by early passage and senescent vascular endothelium is modulated by VPF/VEGF: evidence for senescent endothelial cells in vivo at sites of atherosclerosis. *FASEB J* 2001;**15**:458-66.
20. Kumar A, Kim CS, Hoffman TA, Naqvi A, Dericco J, Jung S, et al. p53 impairs endothelial function by transcriptionally repressing Kruppel-like factor 2. *ATVB* 2011;**31**:133-41.
21. Zgheel F, Alhosin M, Rashid S, Burban M, Auger C, Schini-Kerth VB. Redox-sensitive induction of Src/PI3-kinase/Akt and MAPKs pathways activate eNOS in response to EPA:DHA 6:1. *PLoS One* 2014; 18:9:8: e105102.
22. Niazi ZR, Silva GC, Ribeiro TP, León-González AJ, Kassem M, Mirajkar A, et al. EPA:DHA 6:1 prevents angiotensin II-induced hypertension and endothelial dysfunction in rats: role of NADPH oxidase- and COX-derived oxidative stress. *Hypertens Res* 2017;**40**:966-75.
23. Klymchenko AS, Roger E, Anton N, Anton H, Shulov I, Vermot J, et al. Highly lipophilic fluorescent dyes in nano-emulsions: towards bright non-leaking nano-droplets. *RSC Adv* 2012; 2:31:11876.
24. Bouchaala R, Mercier L, Andreiuk B, Mély Y, Vandamme TF, Anton N, et al. Integrity of lipid nanocarriers in bloodstream and tumor quantified by near-infrared ratiometric FRET imaging in living mice. *J Control Release* 2016;**236**:57-67.
25. Ndiaye M, Chataigneau M, Lobysheva I, Chataigneau T, Schini-Kerth VB. Red wine polyphenol-induced, endothelium-dependent NO-mediated relaxation is due to the redox-sensitive PI3-kinase/Akt-dependent phosphorylation of endothelial NO-synthase in the isolated porcine coronary artery. *FASEB J* 2005;**19**(3):455-457.
26. Abbas M, Jesel L, Auger C, Amoura L, Messas N, Manin G, et al. Endothelial microparticles from acute coronary syndrome patients induce premature coronary artery endothelial cell aging and thrombogenicity: role of the Ang II/AT1 receptor/NADPH oxidase-mediated activation of MAPKs and PI3-kinase pathways. *Circulation* 2017;**135**(3):280-96.
27. Debacq-Chainiaux F, Erusalimsky JD, Campisi J, Toussaint O. Protocols to detect senescence-associated beta-galactosidase (SA-gal) activity, a biomarker of senescent cells in culture and in vivo. *Nat Protoc* 2009;**4**:1798-806.
28. Bou S, Wang X, Anton N, Bouchaala R, Klymchenko AS, Collot M. Lipid-core/polymer-shell hybrid nanoparticles: synthesis and characterization by fluorescence labeling and electrophoresis. *Soft Matter* 2020;**16**(17):4173-81.
29. Rehman AU, Collot M, Klymchenko AS, Akram S, Mustafa B, Vandamme T, et al. Spontaneous nano-emulsification with tailor-made

amphiphilic polymers and related monomers. *Eur J Pharm Res* 2019;**1** (1):27-36.
30. Anton N, Vandamme TF. The universality of low-energy nano-emulsification. *Int J Pharm* 2009;**377**(1–2):142-7.
31. Hoshyar N, Gray S, Han H, Bao G. The effect of nanoparticle size on in vivo pharmacokinetics and cellular interaction. *Nanomedicine (Lond)* 2016;**11**(6):673-92.
32. Kim CS, Jung SB, Naqvi A, Hoffman TA, DeRicco J, Yamamori T, et al. p53 impairs endothelium-dependent vasomotor function through transcriptional upregulation of p66shc. *Circ Res* 2008;**103**:1441-50.
33. Khemais-Benkhiat S, Idris-Khodja N, Ribeiro TP, Silva GC, Abbas M, Kheloufi M, et al. The redox-sensitive induction of the local angiotensin system promotes both premature and replicative endothelial senescence preventive effect of a standardized crataegus extract. *J Gerontol A Biol Sci Med Sci* 2016;**71**:1581-90.
34. Cybulsky MI and Gimbrone MA. Jr. Endothelial expression of a mononuclear leukocyte adhesion molecule during atherogenesis. Science 1991; 251:788–791.
35. Dansky HM, Barlow CB, Lominska C, Kao C, Weinsaft J, Cybulsky MI, et al. Adhesion of monocytes to arterial endothelium and initiation of atherosclerosis are critically dependent on vascular cell adhesion molecule-1 gene dosage. *ATVB* 2001;**21**:1662e7.
36. Cybulsky MI, Iiyama K, Li H, Zhu S, Chen M, Iiyama M, et al. A major role for VCAM-1, but not ICAM-1, in early atherosclerosis. *J Clin Invest* 2001;**107**:1255e62.
37. cHale JF, Harari OA, Marshall D, Haskard DO. Vascular endothelial cell expression of ICAM-1 and VCAM-1 at the onset of eliciting contact hypersensitivity in mice: evidence for a dominant role of TNF-alpha. *J Immunol* 1999;**162**:1648-55.
38. Sans M, Fuster D, Vazquez A, Setoain FJ, Piera C, Pique JM, et al. 123Iodine-labeled anti-VCAM-1 antibody scintography in the assessment of experimental colitis. *Eur J Gastroenterol Hepatol* 2001;**13**:31-8.
39. Alexis F, Pridgen E, Molnar LK, Farokhzad OC. Factors affecting the clearance and biodistribution of polymeric nanoparticles. *Mol Pharm* 2008;**5**:505-15.
40. Hussain A, Samad A, Singh SK, Ahsan MN, Haque MW, Faruk A, et al. Nanoemulsion gel-based topical delivery of an antifungal drug: in vitro activity and in vivo evaluation. *Drug Deliv* 2016;**23**(2):642-57.
41. Nasr M, Nawaz S, Elhissi A. Amphotericin B lipid nanoemulsion aerosols for targeting peripheral respiratory airways via nebulization. *Int J Pharm* 2012;**436**(1–2):611-6.
42. Pawar VK, Panchal SB, Singh Y, Meher JG, Sharma K, Singh P, et al. Immunotherapeutic vitamin E nanoemulsion synergies the antiproliferative activity of paclitaxel in breast cancer cells via modulating Th1 and Th2 immune response. *J Control Release* 2014;**196**:295-306.
43. Saberi AH, Fang Y, McClements DJ. Fabrication of vitamin e-enriched nanoemulsions: factors affecting particle size using spontaneous emulsification. *J Colloid Interface Sci* 2013;**391**:95-102.
44. Kretzer IF, Maria DA, Maranhão RC. Drug-targeting in combined cancer chemotherapy: tumor growth inhibition in mice by association of paclitaxel and etoposide with a cholesterol-rich nanoemulsion. *Cell Oncol* 2012;**35**(6):451-60.
45. Solans C, Morales D, Homs M. Spontaneous emulsification. *Curr Opin Colloid Interface Sci* 2016;**22**:88-93.
46. McClements DJ. Nanoemulsions versus microemulsions: terminology, differences, and similarities. *Soft Matter* 2012;**8**(6):1719-29.
47. Fornaguera C, Grijalvo S, Galán M, Fuentes-Paniagua E, de la Mata FJ, Gómez R, et al. Novel non-viral gene delivery systems composed of carbosilane dendron functionalized nanoparticles prepared from nanoemulsions as non-viral carriers for antisense oligonucleotides. *Int J Pharm* 2015;**478**(1):113-23.
48. Hörmann K, Zimmer A. Drug delivery and drug targeting with parenteral lipid nanoemulsions — a review. *J Control Release* 2016;**223**:85-98.
49. Kilin VN, Anton H, Anton N, Steed E, Vermot J, Vandamme TF, et al. Counterion-enhanced cyanine dye loading into lipid nano-droplets for single-particle tracking in zebrafish. *Biomaterials* 2014;**35**(18):4950-7.
50. Attia MF, Anton N, Chiper M, Akasov R, Anton H, Messaddeq N, et al. Biodistribution of X-ray iodinated contrast agent in nanoemulsions is controlled by the chemical nature of the oily core. *ACS Nano* 2014;**8** (10):10537-50.
51. Wang X, Anton N, Ashokkumar P, Anton H, Fam TK, Vandamme T, et al. Optimizing the fluorescence properties of nanoemulsions for single particle tracking in live cells. *ACS Appl Mater Interfaces* 2019;**11**(14):13079-90.
52. Muthu MS, Leong DT, Mei L, Feng SS. Nanotheranostics — application and further development of nanomedicine strategies for advanced theranostics. *Theranostics* 2014;**4**(6):660-77.
53. Zgheel F, Perrier S, Remila L, Houngue U, Mazzucotelli JP, Morel O, et al. EPA:DHA 6:1 is a superior omega-3 PUFAs formulation attenuating platelets-induced contractile responses in porcine coronary and human internal mammary artery by targeting the serotonin pathway via an increased endothelial formation of nitric oxide. *Eur J Pharmacol* 2019;**15** (853):41-8.
54. Bhatt DL, Steg G, Miller M, Brinton AE, Jacobson TA, Ketchum SB, et al. Cardiovascular risk reduction with icosapent ethyl for hypertriglyceridemia. *N Engl J Med* 2019;**380**:11-22.
55. Khemais-Benkhiat S, Belcastro E, Idris-Khodja N, Park SH, Amoura L, Abbas M, et al. Angiotensin II-induced redox-sensitive SGLT1 and 2 expression promotes high glucose-induced endothelial cell senescence. *J Cell Mol Med* 2020;**24**(3):2109-22.